Quantifying the entropic cost of cellular growth control

Daniele De Martino,[1] Fabrizio Capuani,[2,*] and Andrea De Martino[2,3]

[1]*Institute of Science and Technology Austria, 3400 Klosterneuburg, Austria*
[2]*Soft and Living Matter Laboratory, Institute of Nanotechnology, Consiglio Nazionale delle Ricerche, 00185 Rome, Italy*
[3]*Italian Institute for Genomic Medicine, 10126 Turin, Italy*

Viewing the ways a living cell can organize its metabolism as the phase space of a physical system, regulation can be seen as the ability to reduce the entropy of that space by selecting specific cellular configurations that are, in some sense, optimal. Here we quantify the amount of regulation required to control a cell's growth rate by a maximum-entropy approach to the space of underlying metabolic phenotypes, where a configuration corresponds to a metabolic flux pattern as described by genome-scale models. We link the mean growth rate achieved by a population of cells to the minimal amount of metabolic regulation needed to achieve it through a phase diagram that highlights how growth suppression can be as costly (in regulatory terms) as growth enhancement. Moreover, we provide an interpretation of the inverse temperature β controlling maximum-entropy distributions based on the underlying growth dynamics. Specifically, we show that the asymptotic value of β for a cell population can be expected to depend on (i) the carrying capacity of the environment, (ii) the initial size of the colony, and (iii) the probability distribution from which the inoculum was sampled. Results obtained for *E. coli* and human cells are found to be remarkably consistent with empirical evidence.

I. INTRODUCTION

To a great extent, the physiologic state of a living cell is determined by how a large number of microscopic degrees of freedom subject to noise (nutrient import rates, metabolic reaction fluxes, gene expression levels, etc.) coordinate in response to the sensing of the extracellular conditions. This process ultimately correlates different regulatory variables and constrains the cell's phase space, i.e., the set of viable microscopic configurations. The ensuing reduction of the effective size of the phase space, i.e., the entropy change, can be thought to quantify, roughly speaking, the overall amount of regulation required to correctly modulate the cell's physiology in a given environment. A key idea in this type of scenario is that the fitness level and the strength of regulation necessary to achieve it are tightly linked, with higher fitness being generically associated with stronger regulation [1,2]. Having access to detailed information on genetic and metabolic variables, one may now hope to describe the set of phenotypes selected by regulation, i.e., the physiologically relevant portion of phase space, in terms of the behavior of individual degrees of freedom. On the other hand, a principle-based approach might provide meaningful system-level insights. An important question in this respect is the following: Can one characterize the selected region of the phase space in precise terms?

Bacteria, whose physiology is primarily described by their growth rate (GR), may yield important clues in this respect. Experiments probing bacterial growth at single-cell resolution in fact appraise the significant cell-to-cell variability that accompanies the establishment of a well-defined mean GR across an exponentially growing population [3–5]. Such a heterogeneity reflects, at a phenotypic level, variability in the underlying microscopic configurations and may therefore carry strong regulatory signatures. Recent work has indeed shown that single-cell GR distributions measured for *E. coli* correspond to maximum-entropy distributions of its viable metabolic flux patterns at fixed mean GR, suggesting that metabolic regulation realizes a tradeoff between the high fitness of fast-growing states and the high density of slow-growing ones [6]. By shifting the optimization target from the GR to its entropic costs, the maximum-entropy approach offers a view that is compatible both with the presence of noise in gene expression, which poses fundamental limits to GR optimization [7], and with the idea that the metabolic costs of strictly optimizing growth in fluctuating environments may be prohibitive [5]. The scenario derived so far is however largely incomplete. In particular, besides establishing more connections to experiments, it would be important to devise an interpretation for the Lagrange parameter that constrains the mean GR of maximum-entropy distributions (equivalent to the inverse temperature in a Boltzmann distribution).

Here we expand the maximum-entropy picture by showing the following.

(i) The strength of regulation and the fitness are connected by an extended phase diagram that clarifies how growth repression can be as costly as growth enhancement. After linking to genome-scale models of metabolic networks, this allows us to point to specific mechanisms that cells can exploit to implement those strategies and to qualitatively interpret different types of empirical data.

(ii) The inverse temperature parameter that controls maximum-entropy distributions can be directly connected, in a generic dynamical setting, to the population growth law and, perhaps most unexpectedly, to the initial size of the population, leading to results that are again in agreement with empirical evidence.

This strongly supports the idea that, within the right framework, a statistical physics approach to cellular regulation may provide useful and testable insights into the connections between physiology and regulation.

_____
*Present address: Istituto Nazionale di Fisica Nucleare, Unità di Roma 1, Rome, Italy.

II. BASIC SETUP

Following [6], we focus on metabolic degrees of freedom. We describe each viable metabolism by $\mathbf{v} = \{v_i\}$, representing the vector of metabolic reaction fluxes ($i = 1, \ldots, N$ with N the number of reactions), and by $\lambda(\mathbf{v})$, the GR corresponding to flux configuration $\mathbf{v}$. The space $\mathcal{F}$ of feasible flux vectors $\mathbf{v}$ (the phase space) is formed by the nonequilibrium steady states of the underlying metabolic network, defined by the solutions of $\mathbf{Sv} = \mathbf{0}$, where $\mathbf{S}$ denotes the $M \times N$ stoichiometric matrix (M being the number of chemical species) and where a specific range of variability $[v_i^{\min}, v_i^{\max}]$ is assumed to be given for each v_i based on thermodynamic and kinetic constraints [8]. Maximum-entropy distributions with prescribed mean GR $\langle\lambda\rangle$ over $\mathcal{F}$ are given by

$$p(\mathbf{v}) = \frac{e^{\beta\lambda(\mathbf{v})}}{Z(\beta)} \quad (\mathbf{v} \in \mathcal{F}), \tag{1}$$

where β is the Lagrange multiplier enforcing the constraint $\langle\lambda\rangle = \int_{\mathcal{F}} \lambda(\mathbf{v})p(\mathbf{v})d\mathbf{v}$, while $Z(\beta) = \int_{\mathcal{F}} e^{\beta\lambda(\mathbf{v})}d\mathbf{v}$ is a normalization factor. In the limit $\beta \to 0$ ($\beta \gg 1$), $p(\mathbf{v})$ becomes a uniform distribution over $\mathcal{F}$ [a distribution that concentrates around fastest-growing states with GR $\lambda_{\max} \equiv \max_{\mathbf{v}\in\mathcal{F}} \lambda(\mathbf{v})$]. Following information-theoretic reasoning, for each given β (or $\langle\lambda\rangle$) the effective phase-space volume accessible to the system can be quantified by the entropy $S(\beta) = -\int_{\mathcal{F}} p(\mathbf{v}) \ln p(\mathbf{v})d\mathbf{v}$. In turn, sampling $\mathcal{F}$ by (1) reduces the entropy with respect to the uniform sampling with $\beta = 0$ by a factor I given by [6]

$$I \ln 2 \equiv S(0) - S(\beta) = \beta\langle\lambda\rangle - \int_0^\beta \langle\lambda\rangle d\beta', \tag{2}$$

where $\langle\lambda\rangle$ is a function of β. The above quantity (measured in bits) gauges the effective reduction of the phase space that occurs for any given β and, within the maximum-entropy

scenario, it can be interpreted as the minimal amount of regulation required to establish a given mean GR $\langle\lambda\rangle$. The $\langle\lambda\rangle$ vs I curve obtained from (2) by varying β separates the $(I, \langle\lambda\rangle)$ plane in a feasible region (where I is large enough for the corresponding value of $\langle\lambda\rangle$) and a forbidden region (where I is too small and hence the regulation is insufficient to achieve the desired GR). Reference [6] has characterized this phase diagram for *E. coli* growth in a minimal glucose-limited medium (based on the *i*JR904 genome-scale metabolic network model with $N = 1075$ and $M = 761$ [9]) [see Fig. 1(a) (black line)].

More specifically, maximum-entropy GR distributions lying on this line were found to reproduce different sets of empirical data by fitting a single parameter, with the corresponding values of $\langle\lambda\rangle/\lambda_{\max}$ shown as orange markers in Fig. 1(a).

III. EXTENDED PHASE DIAGRAM

We start by noting that the standard *E. coli* GR in the human gut, corresponding to a doubling time of about 40 h [green marker in Fig. 1(a)], appears to be close to the mean GR obtained for a flat sampling of $\mathcal{F}$ with $\beta = 0$, with both lying close to 1% of $\lambda_{\max}$. Such fitness values are achievable at very small regulatory costs, i.e., for $I \simeq 0$. This however implies that *slower* GRs require some degree of regulation. A slow growth branch in the $(I, \langle\lambda\rangle)$ diagram can be obtained by simply computing (2) for $\beta < 0$. This leads to the red curve in Fig. 1(a) and, in turn, to a second forbidden region at small I and small $\langle\lambda\rangle$, where the amount of regulation I is insufficient to grow at mean rate $\langle\lambda\rangle$ (or, equivalently, where $\langle\lambda\rangle$ is too small for the given value of I). This region provides a direct indication of the entropic costs of growth repression in *E. coli*.

It would be interesting to check whether cells explore the slow branch of the phase diagram as they seem to do with the
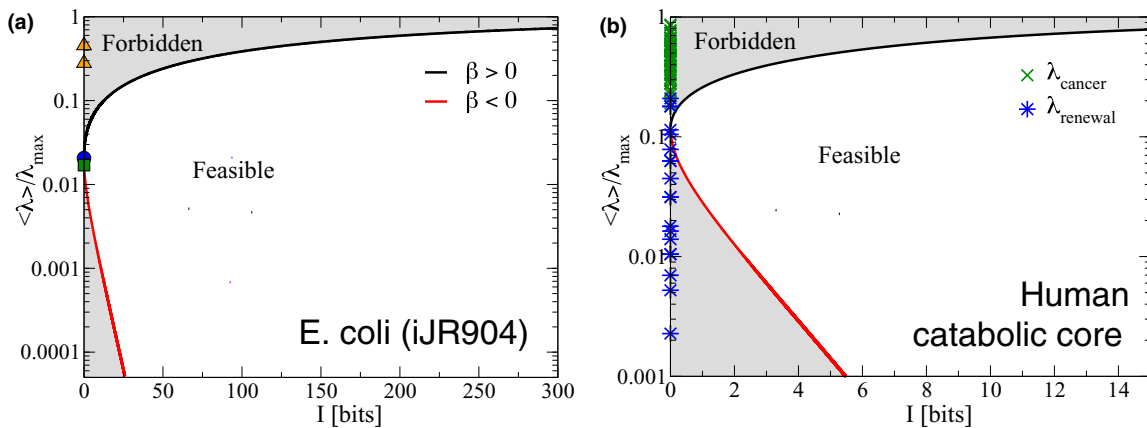

FIG. 1. Both the enhancement ($\beta > 0$) and the suppression ($\beta < 0$) of growth imply regulatory costs in terms of reduced metabolic phase-space accessibility. (a) The $\langle\lambda\rangle/\lambda_{\max}$ versus I trade-off curve computed from the *E. coli* *i*JR904 genome-scale metabolic network model assuming a glucose-limited minimal medium ($\lambda_{\max} = 1/\text{h}$). The blue, green, and orange markers denote the values of $\langle\lambda\rangle/\lambda_{\max}$ (i) found for $\beta = 0$ (i.e., for an unbiased sampling of the feasible space), (ii) estimated for *E. coli* in the human gut (roughly corresponding to a doubling time of 40 h), and (iii) computed in [6] for two sets of GR distributions, respectively, described by the values $\langle\lambda\rangle/\lambda_{\max} \simeq 0.28$ and $\simeq 0.45$. (b) The $\langle\lambda\rangle/\lambda_{\max}$ versus I trade-off curve computed from the human catabolic core network with $\lambda_{\max} \simeq 0.046/\text{h}$, corresponding to a fast GR for cancer cells (doubling time $\simeq 15$ h). Blue and green markers represent, respectively, the estimated renewal rates of various healthy human tissues and the estimated GRs of different types of cancers (data were obtained from [10]). Note that reducing the mean GR by a given factor generically requires a smaller amount of regulation compared to speeding it up by the same factor.

fast branch. Perhaps unsurprisingly, few studies have probed bacteria at very slow growth [11] (although active regulation for dormancy and slow growth occurs in persistent bacteria [12,13]). In human cells (or, more generally, in multicellular systems), on the other hand, growth is usually controlled by a variety of mechanisms that include mechanical (e.g., cell-cell contacts), signaling (e.g., growth factors), and regulatory (e.g., metabolic) pathways. Figure 1(b) displays the $(\langle\lambda\rangle,I)$ phase structure obtained from the carbon catabolic core metabolism of human cells [14] together with the estimated GRs of 61 cancer types (green markers) and the estimated renewal rates of 21 human tissues (blue markers). Remarkably, the mean fitness obtained for $\beta = 0$ is close to separating the two data sets (note that the GR distributions for cancer and healthy tissue cells overlap by less than 10%), suggesting that healthy tissues might indeed probe states close to the slow branch with $\beta < 0$, while cancer cells are more likely associated with growth-enhancing phenotypes with $\beta > 0$.

IV. DIFFERENT STRATEGIES TO ENHANCE AND REPRESS GROWTH

It is instructive to compare the entropy reduction I to the dimension of the feasible space $\mathcal{F}$, equal, in the case of *E. coli* presented in Fig. 1(a), to 233. In order to get close to λ_{max} cells have to invest considerably more than one bit per degree of freedom into regulation, in agreement with the view that GR maximization entails a finer and finer tuning of metabolic reactions (and higher regulatory costs). On the other hand, slowing growth below the unregulated limit only seems to require a fraction of a bit per degree of freedom, compatible with the idea that it is sufficient to act on a few essential reactions to hinder growth. A careful look at solutions selected by the maximum-entropy rule upon varying β (which can be computed as detailed in [6]) sheds light on the regulatory pathways that cells modulate in order to adjust their fitness. Focusing on conditions for which $\lambda_{max} \simeq 0.4$/h (so as to avoid effects due to gene expression costs that set in at faster rates [15]), we see that the flow through futile cycles anticorrelates with the mean GR for $\beta > 0$ [Fig. 2(a)], confirming that the reduction of chemical energy dissipation is a major mechanism of growth maximization [6]. Likewise, increasing β appears to select solutions for which CO_2 is the main carbon compound excreted [Fig. 2(b)], in agreement with the fact that the high-ATP-yield oxidative phenotype should be dominant at the GR values under consideration ($\lambda \lesssim 0.4$/h) [15,16]. On the other hand, no major rearrangement of these pathways is observed for $\beta < 0$, as the mean glucose intake also remains constant [Fig. 2(a)]. This is not surprising in view of the fact that growth suppression appears to require much weaker regulation than growth optimization, as one can see by comparing the slow and fast branches of Fig. 1(a). Interestingly, the only reaction that appears to be significantly modulated along the slow branch of the phase diagram is acetolactate synthase [Fig. 2(a)], a key enzyme for the biosynthesis of branched-chain amino acids in microbes [17,18]. This is reasonable, as limiting amino acid production pathways effectively creates a bottleneck for growth by reducing the rates of protein synthesis.
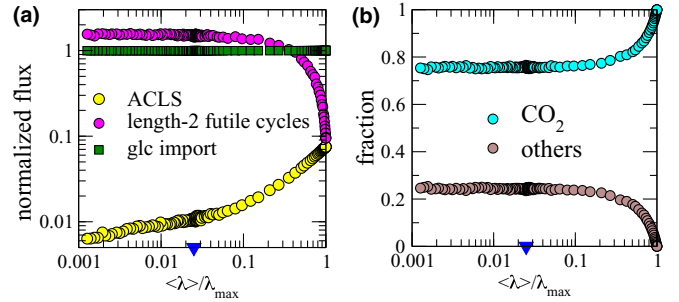

FIG. 2. Different metabolic strategies control growth suppression and enhancement. Modulation of selected metabolic variables with $\langle\lambda\rangle/\lambda_{max}$ for maximum-entropy flux configurations of *E. coli* found under glucose-limited (maximum uptake 4.4 mmol/g_{DW}/h) aerobic conditions with $\lambda_{max} \simeq 0.4$/h. (a) Mean fluxes through acetolactate synthase (ACLS), length-2 futile cycles, and glucose import. (b) Fraction of carbon excreted as CO_2 (cyan) and as other carbon compounds (brown). All fluxes are normalized to the maximum glucose import flux. β increases from $-\infty$ to $+\infty$ as $\langle\lambda\rangle/\lambda_{max}$ grows. The blue triangle marks the value of $\langle\lambda\rangle/\lambda_{max}$ corresponding to $\beta = 0$. Faster mean GRs can be achieved by reducing energy dissipation by futile cycles and improving yields via respiration. Slower rates appear to require the creation of bottlenecks in key pathways like the aminoacid biosynthesis route.

V. PHYSICAL MEANING OF β

This analysis raises the question of whether the parameter β, which in our setting varies from $-\infty$ to $+\infty$, can be seen in more precise terms than simply as a degree of GR optimization (maximization if $\beta > 0$, minimization if $\beta < 0$). To get some physical insight, we analyze a generalization of the standard logistic growth model (see, e.g., [19]). Consider a population of N_0 cells (indexed i) initially planted in a growth medium with finite carrying capacity K and assume (similarly to [20]) that their intrinsic GRs λ_i are sampled independently from a distribution $q(\lambda)$ defined over the feasible space $\mathcal{F}$. Here $q(\lambda)$ simply describes the statistics of the population from which the initial inoculum was obtained. If the finite carrying capacity is the only growth-limiting factor, each of the initial seeds will expand in time according to its intrinsic GR and the number n_i of cells with GR λ_i will evolve in time according to

$$\frac{\dot{n}_i}{n_i} = \lambda_i\left(1 - \frac{N}{K}\right), \quad N(t) = \sum_{i=1}^{N_0} n_i(t), \quad (3)$$

which implies

$$\frac{\dot{N}}{N} = \langle\lambda\rangle_t\left(1 - \frac{N}{K}\right), \quad \langle\lambda\rangle_t = \frac{\sum_i \lambda_i n_i(t)}{\sum_i n_i(t)}. \quad (4)$$

A formal solution of (3) is given by $n_i(t) = e^{\beta(t)\lambda_i}$, with

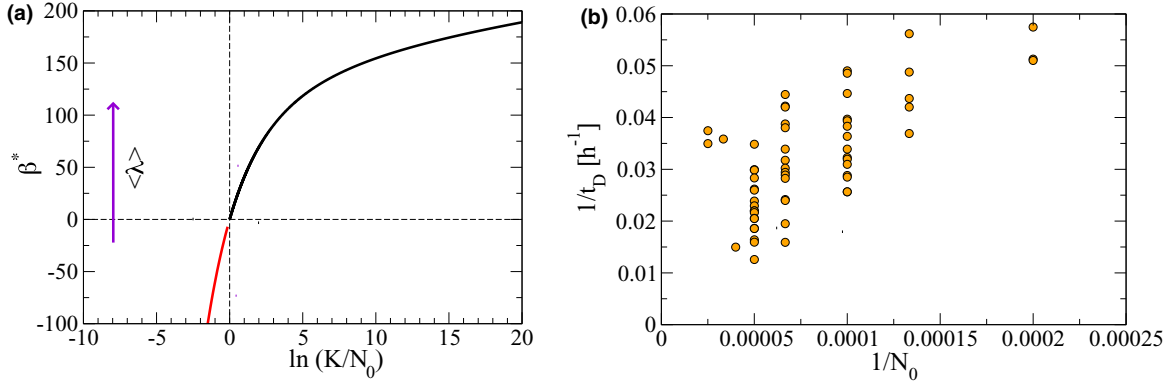$$\beta(t) = t - \frac{1}{K}\int_0^t N(t')dt'. \quad (5)$$

FIG. 3. The asymptotic value of β controlling the phase-space organization of a cell population increases as the initial population size decreases. (a) $\beta^\star$ versus $\ln(K/N_0)$ for the minimal model of population growth described in the text, obtained by solving Eq. (8) for $q(\lambda) \propto (1 - \lambda/\lambda_{\max})^{171}$. Note that $\langle\lambda\rangle$ increases with β. (b) Inverse of the measured doubling times of different cancer cell types (proxies for the mean GRs) as a function of the inverse inoculum size $1/N_0$. Data were obtained from [21].

In turn, for large enough N_0 we can resort to an annealed approximation for $N(t)$, yielding

$$N(t) \simeq N_0 Z(\beta(t)), \quad Z(\beta) = \int q(\lambda)e^{\beta\lambda}d\lambda, \quad (6)$$

so that, from Eqs. (5) and (6),

$$\dot{\beta} = 1 - \frac{N_0}{K}Z(\beta). \quad (7)$$

At stationarity, β settles to a value $\beta^\star$ fixed by the condition

$$Z(\beta^\star) \equiv \int q(\lambda)e^{\beta^\star\lambda}d\lambda = \frac{K}{N_0}, \quad (8)$$

which determines the asymptotic degree of optimization $\beta^\star$ given $q(\lambda)$, the carrying capacity K, and the size of the inoculum N_0. Figure 3(a) shows the solutions obtained for $q(\lambda) \propto (1 - \lambda/\lambda_{\max})^{171}$ (the distribution of λ corresponding to a flat distribution of flux configurations over $\mathcal{F}$ in *E. coli* [6]) as a function of $\ln(K/N_0)$. One can see that $\beta > 0$ for $K > N_0$, while it rapidly becomes more and more negative when $N_0 > K$. In other terms, the asymptotic GR distribution is of the maximum-entropy type and concentrates on growth-suppressing states with $\beta < 0$ for stressed initial conditions for which the initial size of the population N_0 exceeds the carrying capacity K. (Note that the picture obtained for $N_0 > K$ may be relevant for a more realistic class of stresses than excess initial population; see, e.g., [22].)

The important role played by N_0 (or, more precisely within the model discussed above, by N_0/K) in determining how a population of cells will asymptotically distribute over the phase space $\mathcal{F}$ seems to represents a rather counterintuitive prediction. Within the above model, the existence of a finite β linked to N_0 is simply due to the fact that, if N_0 values of λ are sampled from a distribution $q(x) = (1 + a)(1 - x)^a$ (with $x \equiv \lambda/\lambda_{\max}$ the relative GR), then on average cells will have values of x lying below

$$x_c(N_0) = 1 - [(1 + a)N_0]^{-1/a}. \quad (9)$$

This, however, corresponds to a value of β given by $\beta_c = a[(1 + a)N_0]^{1/a}$. In other words, the maximum β achievable by a population evolving as in (3) is determined by N_0 [and

by the specifics of $q(\lambda)$]. It is in our view remarkable that the decrease of $\langle\lambda\rangle$ upon increasing N_0 [see Fig. 3(a)] is consistent with the increase of doubling times with N_0 found for various cancers *in vitro*, at least for small enough N_0 [see Fig. 3(b)]. Experiments probing the slow-growth regimes may clarify if *E. coli* cells saturate the slow branch in Fig. 1(a) as they seem to do with the fast branch.

VI. CONCLUSION

The setup presented here combines a standard statistical physics view with genomewide knowledge of cell metabolism to address, at a general level, the question of how a population of exponentially growing cells organizes in its phase space $\mathcal{F}$. Complementing the standard view that focuses on the molecular determinants of growth control [23], we propose a system-level approach whose key idea is that both the fitness (i.e., the mean GR) and the density of metabolic states in $\mathcal{F}$ contribute to the establishment of well-defined single-cell distributions of metabolic phenotypes, leading to a maximum-entropy description of cellular metabolic states. Defining the amount of regulation required to set a given mean GR as the corresponding phase-space entropy reduction, we found an explicit relationship linking regulation and fitness and quantitatively showed that slow growth requires active regulation. Applying the maximum-entropy idea to genome-scale models, different regulatory tuners were identified that cells can act upon in order to control their GR from very fast to very slow. Finally, we proposed a minimal theoretical interpretation for the key parameter of our maximum-entropy theory based on the dynamics of population growth. Ultimately, it is in our view the exponential character of the population growth law that leads to maximum-entropy distributions over $\mathcal{F}$. This analysis has also brought to light the possibly key role played by the parameter N_0, i.e., the initial size of a cellular population. Despite its basic crudeness, our theory provides quantitative information on the interplay between regulation and growth in different cell types and is in qualitative agreement with known empirical data. The maximum-entropy approach therefore seems to provide once more [24] concepts to analyze the organization and performance of living systems

in a statistical physics perspective. Experiments probing slow-growth regimes could clarify if cells saturate the slow branches shown in Figs. 1(a) and 1(b) as they seem to do with the fast branch, at least for *E. coli* [6]. Perhaps more importantly, though, the maximum-entropy scenario discussed here could be further validated by metabolic data at single-cell resolution, e.g., regarding enzyme levels, metabolite levels, and metabolic fluxes. Advances in single-cell metabolomics may therefore play a key role in unraveling novel system-level organization principles in living cells and populations [25]. On a more abstract level, it would be interesting to extend the simple population growth model presented here, specifically to clarify

the conditions leading to $\beta < 0$ as opposed to $\beta > 0$. Most notably, the explicit inclusion of the interplay between the cell population and an environment-borne nutrient is likely to provide important insight in this respect.

[1] S. F. Taylor, N. Tishby, and W. Bialek, Information and fitness, arXiv:0712.4382.

[2] W. Bialek, *Biophysics: Searching for Principles* (Princeton University Press, Princeton, 2012), Sec. 6.3.

[3] S. Taheri-Araghi, S. Bradde, J. T. Sauls, N. S. Hill, P. A. Levin, J. Paulsson, M. Vergassola, and S. Jun, Cell-size control and homeostasis in bacteria, Curr. Biol. **25**, 385 (2015).

[4] A. S. Kennard, M. Osella, A. Javer, J. Grilli, P. Nghe, S. J. Tans, P. Cicuta, and M. C. Lagomarsino, Individuality and universality in the growth-division laws of single *E. coli* cells, Phys. Rev. E **93**, 012408 (2016).

[5] M. Wallden, D. Fange, E. G. Lundius, Ö. Baltekin, and J. Elf, The synchronization of replication and division cycles in individual *E. coli* cells, Cell **166**, 729 (2016).

[6] D. De Martino, F. Capuani, and A. De Martino, Growth against entropy in bacterial metabolism: The phenotypic trade-off behind empirical growth rate distributions in *E. coli*, Phys. Biol. **13**, 036005 (2016).

[7] D. J. Kiviet, P. Nghe, N. Walker, S. Boulineau, V. Sunderlikova, and S. J. Tans, Stochasticity of metabolism and growth at the single-cell level, Nature (London) **514**, 376 (2014).

[8] J. D. Orth, I. Thiele, and B. Ø. Palsson, What is flux balance analysis? Nat. Biotechnol. **28**, 245 (2010).

[9] J. L. Reed, T. D. Vo, C. H. Schilling, and B. O. Palsson, An expanded genome-scale model of *Escherichia coli* K-12 (*i*JR904 GSM/GPR), Genome Biol. **4**, R54 (2003).

[10] bionumbers.org.

[11] W. Chesbro, T. Evans, and R. Eifert, Very slow growth of Escherichia coli., J. Bacteriol. **139**, 625 (1979).

[12] A. Harms, E. Maisonneuve, and K. Gerdes, Mechanisms of bacterial persistence during stress and antibiotic exposure, Science **354**, aaf4268 (2016).

[13] J. L. Radzikowski, S. Vedelaar, D. Siegel, Á. D. Ortega, A. Schmidt, and M. Heinemann, Bacterial persistence is an active σ^S stress response to metabolic flux limitation, Mol. Syst. Biol. **12**, 882 (2016).

[14] F. Capuani, D. De Martino, E. Marinari, and A. De Martino, Quantitative constraint-based computational model of tumor-to-stroma coupling via lactate shuttle, Sci. Rep. **5**, 11880 (2015).

[15] M. Mori, T. Hwa, O. C. Martin, A. De Martino, and E. Marinari, Constrained allocation flux balance analysis, PLoS Comput. Biol. **12**, e1004913 (2016).

[16] D. Molenaar, R. van Berlo, D. de Ridder, and B. Teusink, Shifts in growth strategies reflect tradeoffs in cellular economics, Mol. Syst. Biol. **5**, 323 (2009).

[17] F. E. Dailey and J. E. Cronan, Jr., Acetohydroxy acid synthase I, a required enzyme for isoleucine and valine biosynthesis in *Escherichia coli* K-12 during growth on acetate as the sole carbon source, J. Bacteriol. **165**, 453 (1986).

[18] S. Garg, L. Yang, and R. Mahadevan, Thermodynamic analysis of regulation in metabolic networks using constraint-based modeling, BMC Res. Notes **3**, 125 (2010).

[19] J. Baranyi and T. A. Roberts, A dynamic approach to predicting bacterial growth in food, Int. J. Food Microbiol. **23**, 277 (1994).

[20] S. Franz, L. Peliti, and M. Sellitto, An evolutionary version of the random energy model, J. Phys. A **26**, L1195 (1993).

[21] dtp.cancer.gov/discovery_development/nci-60/cell_list.htm.

[22] K. M. Pruitt and D. N. Kamau, Mathematical models of bacterial growth, inhibition and death under combined stress conditions, J. Ind. Microbiol. **12**, 221 (1993).

[23] W. Palm and C. B. Thompson, Nutrient acquisition strategies of mammalian cells, Nature (London) **546**, 234 (2017).

[24] T. Mora, A. M. Walczak, W. Bialek, and C. G. Callan, Jr., Maximum entropy models for antibody diversity, Proc. Natl. Acad. Sci. USA **107**, 5405 (2010).

[25] R. Zenobi, Single-cell metabolomics: Analytical and biological perspectives, Science **342**, 1243259 (2013).